

Belo Horizonte, Brazil; September 09-14, 2018

EVALUATION OF DELTA WING EFFECTS ON THE STEALTH-AERODYNAMIC FEATURES FOR NON-CONVENTIONAL FIGHTER AIRCRAFT

Pedro David Bravo-Mosquera*, Alvaro Martins Abdalla*, Fernando Martini Catalano*

* Department of Aeronautical Engineering, São Carlos Engineering School, University of São Paulo, Brazil

Keywords: RCS, Delta wing, Wave drag, CFD

Abstract

Survivability and maneuverability have become the major design factors in the development of future military aircraft with stealth ability. The intake fully integrated into the fuselage combined with an S-duct diffuser provide line-ofsight blockage of the engine blades, satisfying the requirement of low signature, lightweight and low drag for the next generation of air-This paper aims to provide an insight about radar cross section (RCS) and aerodynamics of several delta platforms that would help the need and amount of RCS suppression to escape detection from surveillance radars and reduce wave drag. The stealth characteristics were modeled using POFACETS software, which enabled the prediction of the RCS targets using triangular facets. The aerodynamic characteristics were evaluated through the investigation of the wave drag phenomena of each delta platform, using a linearized mathematical model to intercept the aircraft cross sectional area regarding the angle of the Mach cone produced. These results were compared with computational fluid dynamics (CFD) simulations, which were performed using Reynolds-Averaged-Navier-Stokes (RANS) equations, coupled with the Shear Stress Transport (SST) turbulence model. Results showed that the stealth and aerodynamic characteristics of a non-conventional fighter aircraft can be optimized through integration analysis processes.

1 General Introduction

The conception of non-conventional fighter aircraft with the aim of achieving a certain performance or operational improvement is undoubtedly, one of the most important objectives of the aeronautical engineering. These improvements involve: drag reduction, radar cross section (RCS) reduction, noise reduction, shortening of take-off and landing distances, increase of aerodynamic efficiency, armament weight increase, among others. Therefore, the analysis of delta platforms effects on the stealth-aerodynamic characteristics are essential to upgrade the conceptual design of this kind of aircraft.

During the design of a fighter aircraft, there are different techniques to reduce the RCS; the most common is by modeling the surface of the aircraft in such a way that radar waves be dispersed away from radar receiver. However, its exceptional form, manufactured by flat boards, are aerodynamically unstable [1]. For that reason, in this work was considered another approach to aircraft design, which refers to the use of a thin airfoil and a tailless delta wing design, with a top mounted intake and single vector engine hidden within the fuselage, highlighting a smooth combination of the external surfaces and improving the survivability and maneuverability aircraft capabilities.

The delta platform study continues to be a

subject of interest for most aircraft designers, due to its advantages of significant reduction in structural weight, drag, and cost. The weight reduction and drag over traditional aircraft is achieved by eliminating the empennage surface. Therefore, the cost reduction comes by virtue of the improved lift to drag and consequently reduced fuel consumption [2].

This paper conducts studies of theoretical models developed for the purpose of demonstrating the importance of the shape in the RCS and wave drag of a non-conventional aircraft. The configurations have the same airfoil, fuselage length and intake location, however, five different delta platforms were designed in order to determine the configuration that best adjusts to the mission constraints, performing an equilibrium between low RCS and aerodynamics.

2 Delta wing platforms

Delta wings suffer from some undesirable characteristics such as notably flow separation at high angles of attack (swept wings have similar problems), and high drag at low speeds [3]. This originally limited them primarily to high-speed, high-altitude interceptor roles. Since then the delta design has been modified in different ways to overcome some of these problems. These include: Ogival delta wing, Standard delta with LEX (Leading Edge Extensions), Compound delta wing, Canard delta wing, Double delta wing (Fig. 1).

In this paper, the RCS of several planform shapes of delta wings are studied, when the planform has the same reference area, the same airfoil at a constant angle of Attack and wing dihedral angle at zero degrees. To ensure this, the Aspect Ratio (AR) and taper ratio (λ) are varied so that all the examples have an equal area but are representative of the actual airplanes. It should be noted that conceptual 3D digital models are designed in SOLIDWORKS software.

The non-conventional fighter aircraft conceptually designed for this article is a kind of operational aircraft with a single seat, single vector engine and dorsal intake configuration, since this

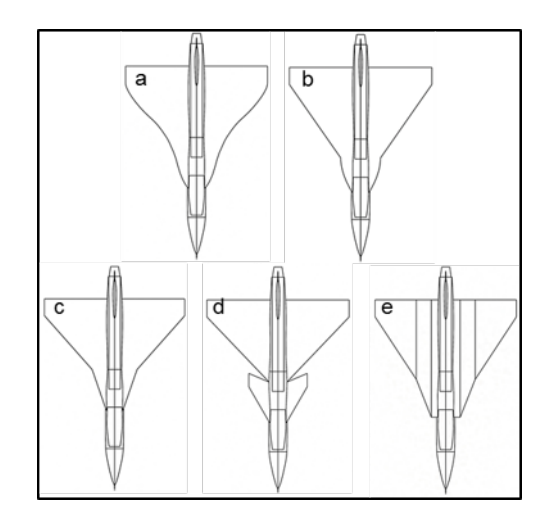


Fig. 1 Delta wing planform: (a) Ogival delta, (b) Standard delta with LEX, (c) Compound delta, (d) Canard delta, (e) Double delta.

configuration represents a low radar signature by integrating the engine into the aircraft using an S-duct diffuser, which prevents direct radar line-of-sight to the engine face. (Table 1).

Table 1 Basic parameters of the conceptual design.

Parameter	Value
Length	14.6 m
Height	4.5 m
MTOW	14000 kg
Empty weight	6600 kg
Weapons weight	4000 kg
Range	3000 km
Service ceiling	16500 m
Wing loading	$415 \ kg/m^2$
T/W ratio	0.92
Engine	Pratt & Whitney F100-229
Main airfoil wing	NACA64a204

More specific details are found in Bravo-Mosquera [4].

3 Radar cross section

The RCS is a measure of the ability of a target to reflect radar energy, affecting the maximum range at which this target is detected by a radar set [5]. Concerning monostatic radars, RCS can be defined as the power scattered from a target to a certain direction, when the target is illumi-

nated by electromagnetic radiation [6, 7]. Therefore, a larger value of this measure means high detectability by radar. Summarizing into a single term, monostatic RCS, in terms of electric field is:

$$\sigma = \lim_{r \to \infty} 4\pi r^2 \frac{\mid E_S \mid^2}{\mid E_I \mid^2} \tag{1}$$

where r is the distance between the target and the radar, E_S and E_I are the scattered and incident electric fields, respectively.

The Eq. 1 is valid when the target is illuminated by a plane wave. It should be noted that RCS values must be in square meters. However, due to the large range of values, it is usually given in a decibel scale. The conversion of scales can be presented as Eq. 2.

$$dBSm = 10log\left(\frac{\sigma}{1m^2}\right) \tag{2}$$

Radar cross section is a function of many factors which include the target configuration and its material composition, frequency or wavelength, transmitter and receiver polarizations, and the target aspect (angular orientation of the target) relative to the radar [8].

3.1 POFACETS software application

The POFACETS code is a MATLAB application based on the Physical Optics (PO) method to predict the RCS targets (3D CAD models) using triangular facets [8].

PO is a high frequency approximation that provides adequate results for electrically large targets, in the specular direction, by approximating the induced surface currents. The PO currents are integrated over the illuminated portions of the target to obtain the scattered far field, while setting the current to zero over the shadowed portions. Since the current is set to zero at the shadow boundary, the computed field values are inaccurate at wide angles and in the shadow regions. Furthermore, surface waves, multiple reflections and edge diffractions are not taken into account. However, the simplicity of this approach ensures low computational overhead [9].

Table 2 No. of cells for the different delta wing planform.

Delta wing	Area $[m^2]$	No. of cells at 10 GHz
Ogival	34.27	13549
LEX	34.12	13254
Compound	34.10	12459
Canard	34.01	11509
Double	34.35	11492

In this paper, a two-step approach is proposed in order to predict the RCS for each configuration. Firstly, a 3D model of the targets are created and refined according to available data, i.e. fuse-lage length, intake position and wing planform. Then, the POFACETS code is employed.

For any signature shape, the low observability of aircraft depends on the wavelength. Therefore, it is one of the factors that determine the area of the radar cross-section. This work only calculates RCS considering high frequencies. The reason of this is that radar operating in L-band (lower frequencies) produces wavelengths with comparable size to the aircraft itself and should exhibit scattering in the resonance region rather than the optical region [10].

3.2 Model description

Five aircraft of different delta wing shape are modeled in SOLIDWORKS and discretized in triangular facet surfaces using the ACIS Solids module of POFACETS. (see Fig. 2).

Table 2 lists the number of surface cells used for discretization for the surface area considered.

The main objective is to study the RCS measurements which aim to determine effective area responsible for backscatter when hit by a radar wave. In this way, some assumptions are required. As the radar is only monostatic case, the target is involved with the high frequency (X-Band) range.

Based on the assumptions described above, the frequency bands chosen in this analysis follow the guidelines of the Federal Radar Spectrum Requirements [11].

On the polar coordinates of the RCS charac-

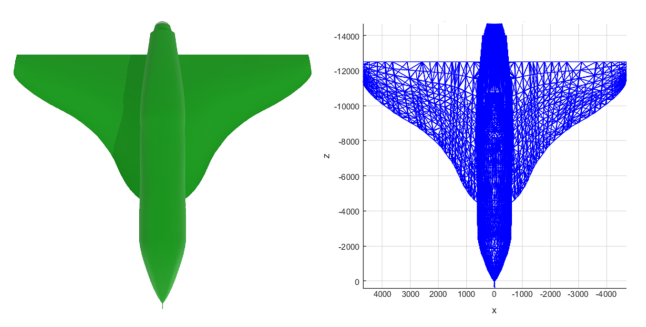


Fig. 2a. Ogival delta.

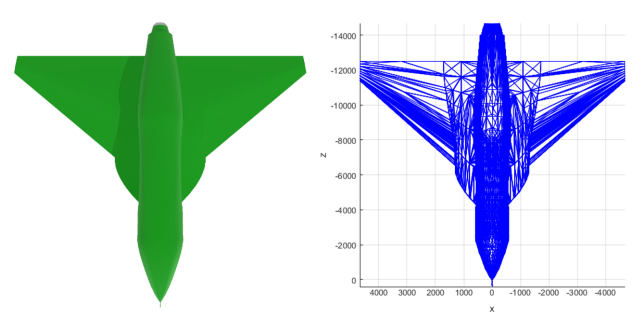


Fig. 2b. Standard delta with LEX.

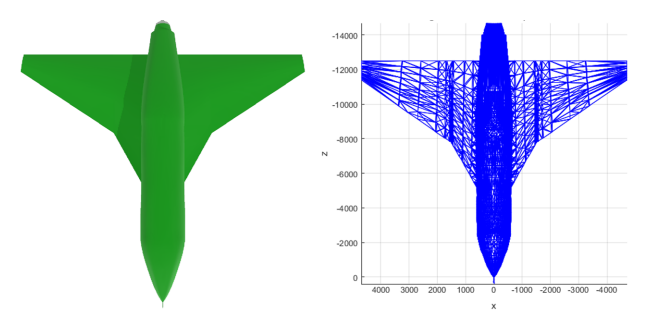


Fig. 2c. Compound delta.

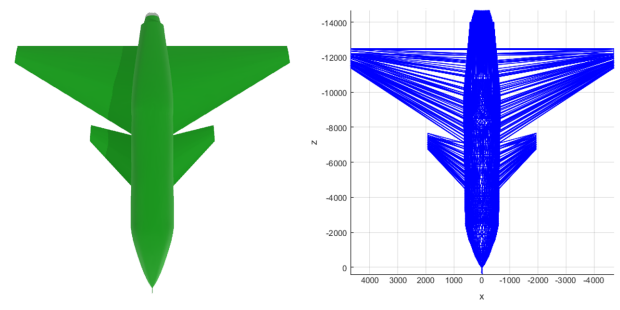


Fig. 2d. Canard delta.

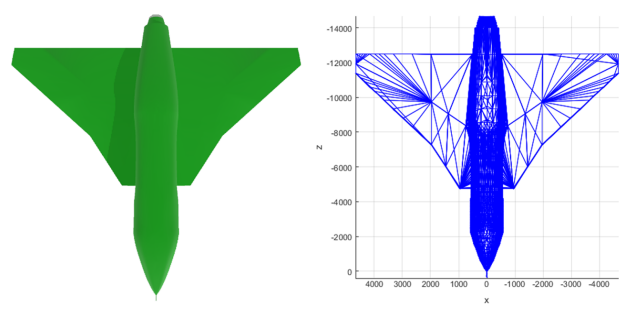


Fig. 2e. Double delta.

Fig. 2 Triangular facet surface scheme of delta wing planform.

teristics, the azimuth angle (Θ) is set between 0° to 180° . The elevation angle (Φ) is set at 0° in order to nearby RCS analysis in front of the aircraft. It should be noted that no special materials were used in the coating of the configurations, therefore, materials application to reduce wavelength is beyond the scope of this research.

4 Wave drag estimation

The wave drag of the configurations was calculated based on the method proposed by Raymer [12]. This uses several empirical tools and takes into account both, the wing and fuselage dimensions using a plane average method and Mach cone method [13]. The following steps are followed to obtain the areas to calculate the wave drag.

- Use Computer Aided-Design tools to create the configurations.
- Create Mach cone planes defined by its respective Mach angle.
- Intersect the geometry of the configurations with the Mach cone planes regarding the direction of flight (Fig. 3).

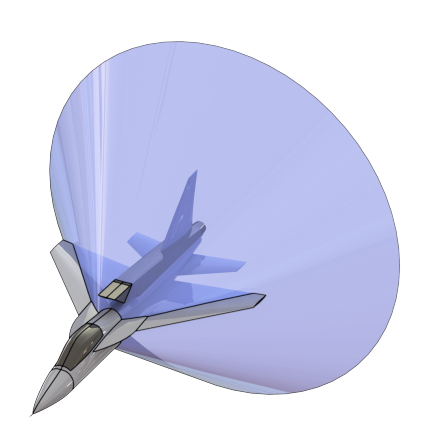


Fig. 3 Mach cone plane intersection with aircraft geometry.

 Normalize the obtained area by the intersection of the configurations with the Mach cone plane.

EVALUATION OF DELTA WING EFFECTS ON THE STEALTH-AERODYNAMIC FEATURES FOR NON-CONVENTIONAL FIGHTER AIRCRAFT

• Create a point in the Z-direction in order to obtain the profile of the area distribution at each section of the models, as shown in Fig. 4.

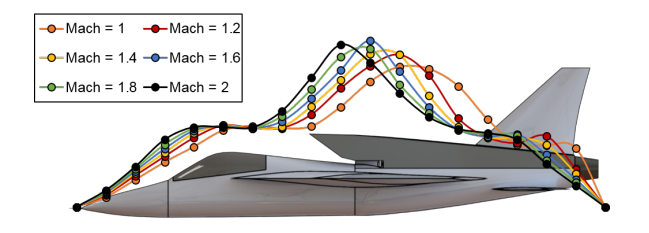


Fig. 4 Effective Mach cone area distribution for different Mach numbers ranging from 1 to 2.

• Calculate the wave drag coefficient (C_{D_W}) in relation to the area distribution obtained.

For preliminary wave drag analysis at $Mach \ge 1.2$, a correlation to the Sears-Haack body wave drag is presented in Eq. 3.

$$C_{D_W} = E_{WD} \left[1 - 0.386(M - 1.2)^{0.57} \left(1 - \frac{\pi \Lambda_{LE}^{0.77}}{100} \right) \right] \cdots \left(\frac{D}{q} \right)_{Sears-Haack}$$
(3)

where E_{WD} is defined by the correlation between the aircraft and the Sears-Haack body wave drag; also known as empirical wave drag efficiency factor. Λ_{LE} is the wing leading edge sweep angle, given in degrees, and $(D/q)_{wave}$ is the minimum possible wave drag for any closedend body of the same length and total volume, given by Eq. 4.

$$\left(\frac{D}{q}\right)_{wave} = \frac{9\pi}{2} \left(\frac{A_{MAX}}{l}\right)^2 \tag{4}$$

where A_{MAX} is the maximum cross-sectional area, determined from the aircraft volume-distribution plot, and l is the overall aircraft length.

Based on Hayes [15], the shock wave drag for bodies immersed in transonic speeds only depends on the longitudinal area distribution of the system as a whole. Therefore, the Theodore von Kármán formula for slender bodies of revolution (Eq. 5) was used for Mach between 0.8 to 1.2.

$$C_{DW} = \frac{\rho V^2}{4\pi} \int_{-x_0}^{x_0} \int_{-x_0}^{x_0} S''(x) S''(x_1) Log|x - x_1| dx dx_1 \quad (5)$$

where S(x) represents the cross-sectional area intercepted by a perpendicular plane to the freestream, at a distance x from the tip of the body.

5 CFD approach

CFD Simulations were carried out using the commercial code ANSYS-FLUENT, which solves the compressible Reynolds-Average-Navier-Stokes (RANS) equations using a 2nd order finite volume scheme. The solver uses the Shear Stress Transport (SST) turbulence model for all of the simulations. For the computational domain, no-slip adiabatic wall boundary conditions are imposed on the solid walls. Specified inlet velocities are imposed at inlet boundary regarding the flying Mach. The outlet condition was imposed with no pressure gradient and walls were set as non-friction (ideal) walls.

Multi-block structure mesh is generated by Meshing ANSYS ICEM-CFD software. Figure 5 shows a detail view of the surface grids around the configurations. A series of grid with increasing resolution is used to determine the grid sensitivity involved in the numerical study. The final grid of 5.8 million elements is adopted in the subsequent numerical analysis.

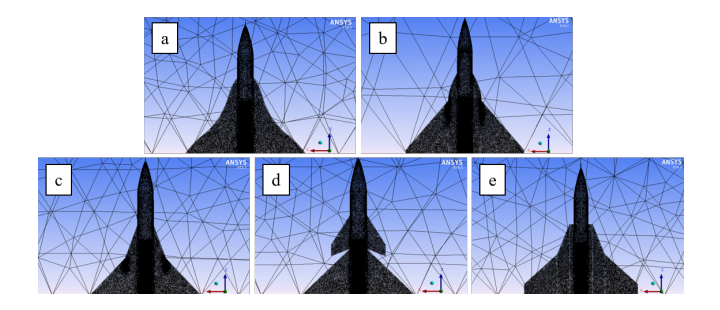


Fig. 5 Mesh structure for delta wing configurations: (a) Ogival delta, (b) Standard delta with LEX, (c) Compound delta, (d) Canard delta, (e) Double delta.

6 Results and Discussion

In this section, results are divided in two subsections. First, the RCS analysis is presented and discussed. Then, the analytic wave drag estimation is compared to CFD simulations.

6.1 Radar cross section

The monostatic RCS is computed, where transmitter and receiver are co-located. As mentioned above, configurations are approximated by arrays of triangles (facets), and the scattered field of each triangle is computed as isolated. Multiple reflections, edge diffraction and surface waves are not considered. All parameters are set to default values, unless otherwise specified.

The RCS of the configurations was computed for a radar transmitting at 10 GHz (X-Band), emulating a typical aircraft fire control radar. The RCS pattern shown in the following figures corresponds to polar plot of all RCS configurations, observed from the same level (Θ ranging from 0^o to 180^o and Φ set at 0^o).

The configuration with lowest RCS signature was the standard delta with LEX, with values between -10 and 40 dBsm (see Fig. 6). In this polar plot, it is observed that the peaks occur in 0 and 180 degrees with a signature of 40 dBsm. In the same way, in the region between 100 and 120 degrees, the RCS value was 10 dBsm. For other regions, the RCS signature goes down to values close to -10 dBsm.

On the other hand, the Double delta configuration presents its maximum peaks at 0 and 180 degrees of around 55 dBsm and, in the region between 100 and 120 degrees with value around 12 dBsm. For other regions, the RCS signature goes down to values close to 0.0 dBsm (see Fig. 7).

Finally, Ogival delta (8), Compound delta (9) and Canard delta (10) presented similar signatures, with peak values at 0 and 180 degrees of around 55 and 60 dBsm. Furthermore, for 20 and 160 degrees, the average RCS signature was 20 dBsm.

Since all configurations have the same fuselage, dorsal intake and vertical empennage, the explanation of the RCS signature reduction for the Standard delta with LEX and Double delta is due to the planform of the configurations. Note that Standard delta with LEX and Double delta have different leading edges sweep, which enhances survivability by the non-uniform fringe surfaces. By last, canards can potentially have poor stealth characteristics due to their large and angular surfaces that tend to reflect radar signals forwards.

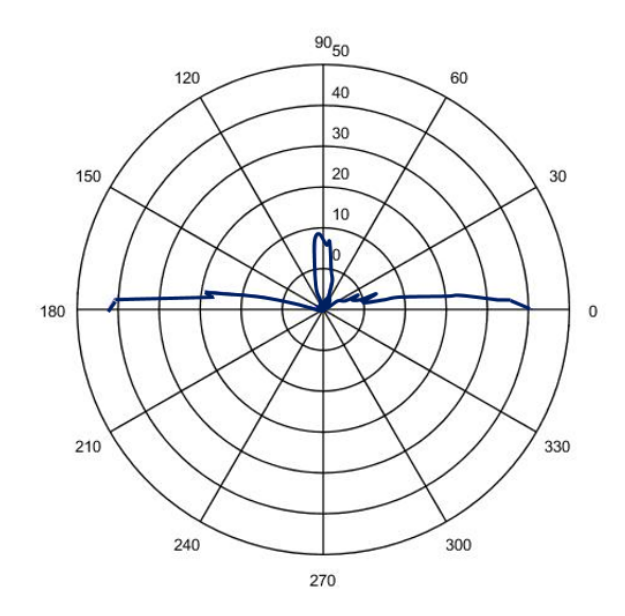


Fig. 6 LEX configuration, RCS characteristic curve.

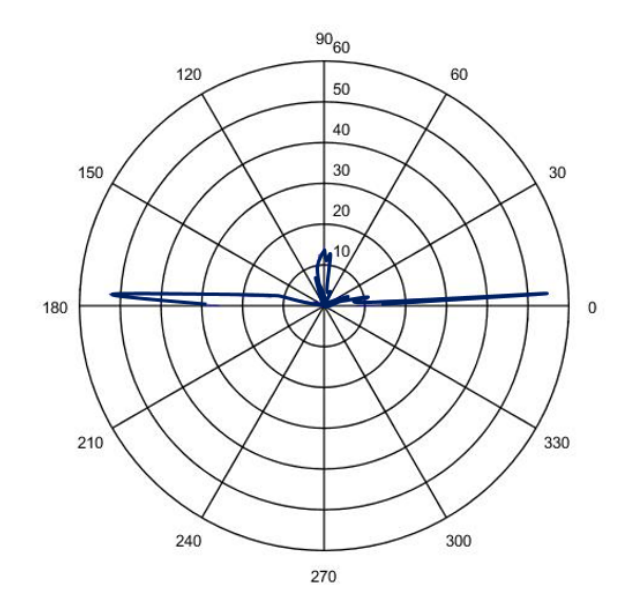


Fig. 7 Double configuration, RCS characteristic curve.

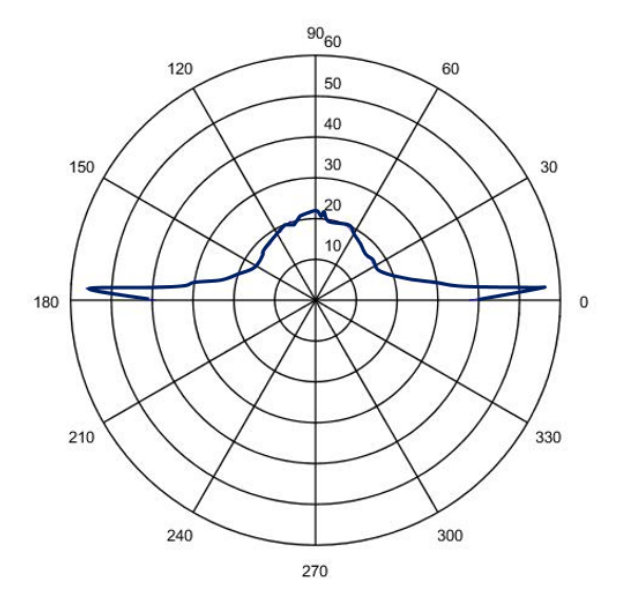


Fig. 8 Ogival configuration, RCS characteristic curve.

Figure 11 shows the linear plot of the RCS analysis, where are compared all the configurations tested. This figure allows to verify that for this specific case, the standard delta with LEX was the configuration with the lowest RCS signature. However, for more accurately results, it is still necessary to evaluate more azimuth and elevation angles on each configuration.

Table 3 summarizes the results obtained in the RCS analysis.

Table 3 RCS signature results

Table 5 Res signature results.		
Delta wing	RCS min-max [dBsm]	
Ogival	20 - 55	
LEX	-10 - 40	
Compound	20 - 60	
Canard	20 - 60	
Double	0 - 55	

6.2 Wave drag estimation

In this section, the analytical wave drag calculations are compared to CFD simulations. Figure 12 shows the wave drag coefficient (C_{DW}) in function of Mach number, between the analytical model presented and the CFD simulation for the five configurations evaluated. It was observed that for Mach = 1, the analytical C_{DW} were higher

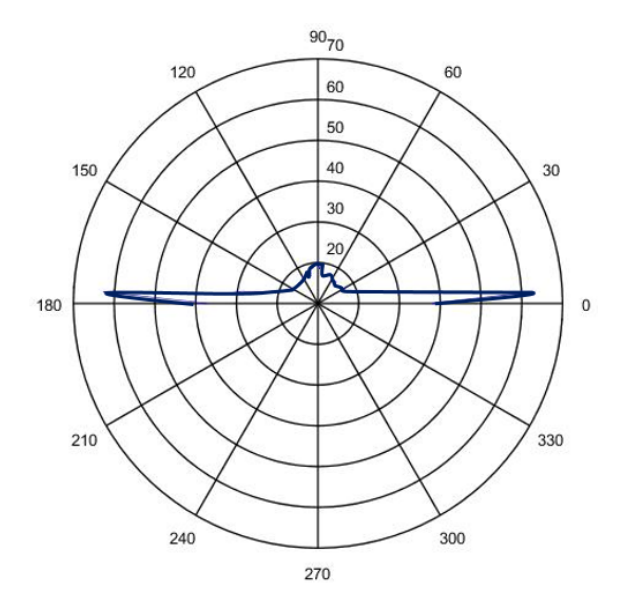


Fig. 9 Compound configuration, RCS characteristic curve.

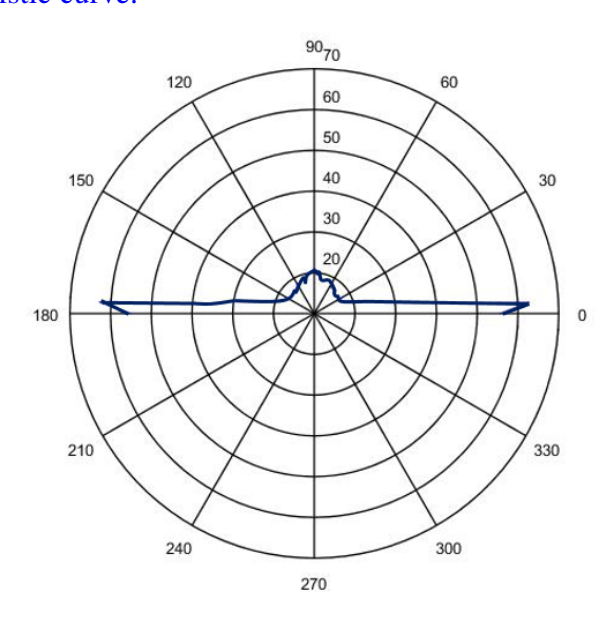


Fig. 10 Canard configuration, RCS characteristic curve.

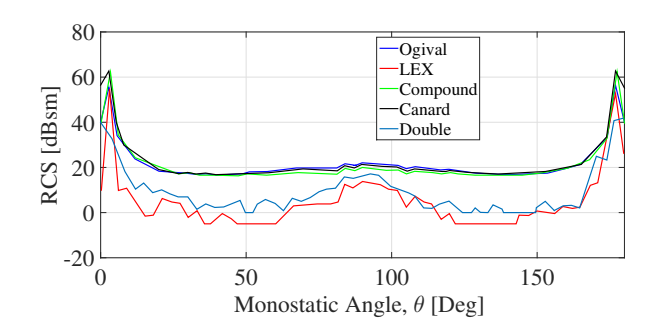


Fig. 11 Comparison of linear plot, RCS characteristic curves.

than CFD. However, for Mach > 1, the analytical C_D were reduced considerably.

These results are likely a product of the imprecision of the analytical calculations to evaluate wave drag coefficients in transonic velocities. Nevertheless, the CFD wave drag values were higher for supersonic velocities, mainly due to the CFD simulations allowed to create conditions closer to reality, at which not only the cross section is considered, whereas also the compressibility effects. Meanwhile, it was observed that both curves presented the same behavior, where the average margin of error for the five configurations in the six velocities evaluated was 1.93%, which allowed to conclude that the analytical model developed were reliable.

The analytical wave drag comparison for the five configurations tested are depicted in Fig. 13. It is evident that the Ogival delta configuration presents a reduced wave drag coefficient at Mach = 1. However, for Mach = 2, the wave drag coefficient is increased. This result is a consequence of the relative increase of the cross-sectional area of the Ogival configuration with the Mach cone plane. LEX and Compound configurations are the models with the lowest wave drag at all evaluated velocities. However, Canard and Double delta configurations presented the highest wave drag values.

Finally, similar results were obtained in the numerical wave drag comparison for the five configurations (see. Fig. 14).

7 Conclusions

In the present research, the stealth and aerodynamic characteristics of five delta wing configurations in the same aircraft geometry were analyzed.

The main results suggested that stealth-aerodynamic characteristics of the non-conventional fighter aircraft can be based on the analysis process of the integration of stealth aircraft conceptual design and aerodynamic analysis.

The RCS calculations presented adequate results for preliminary stealth studies. However,

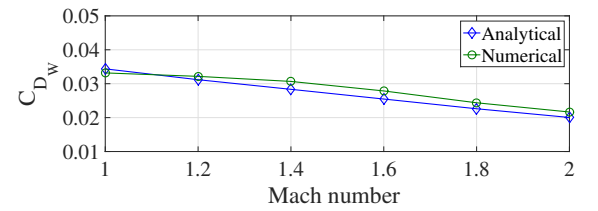


Fig. 12a. Ogival delta.

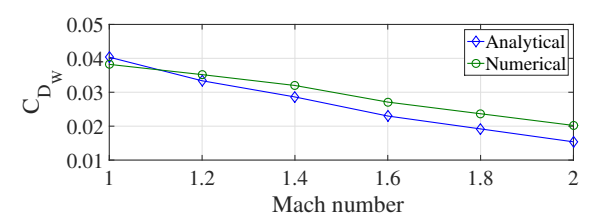


Fig. 12b. Standard delta with LEX.

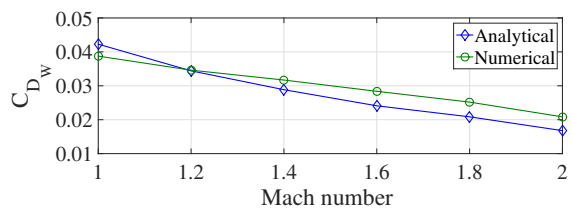


Fig. 12c. Compound delta.

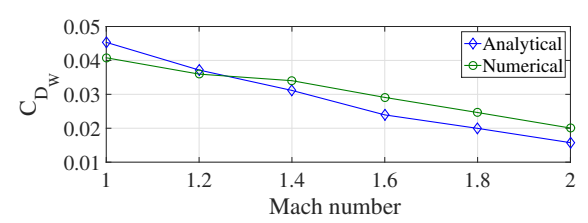


Fig. 12d. Canard delta.

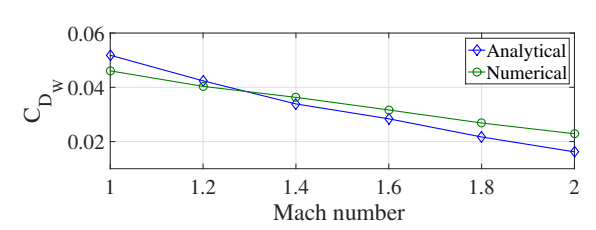


Fig. 12e. Double delta.

Fig. 12 Wave drag coefficient comparison, analytical and numerical methods.

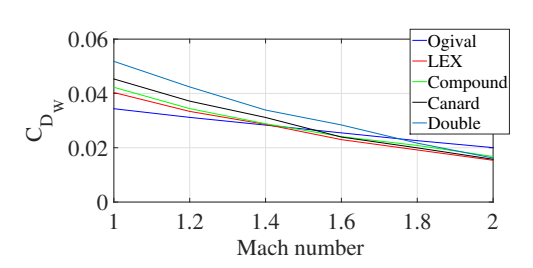


Fig. 13 C_{D_W} Vs Mach number, analytical calculations.

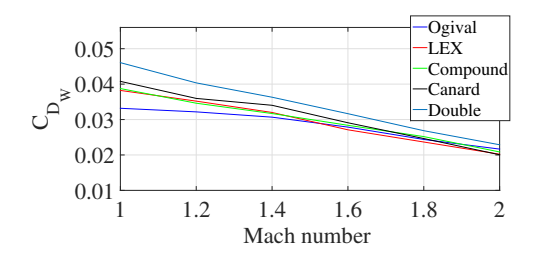


Fig. 14 C_{D_W} Vs Mach number, numerical simulations.

more azimuth and elevation angles are still necessary for a detailed analysis of the presented designs. On the other hand, the aerodynamic analysis has been successfully used to evaluate the aerodynamic drag of transonic and supersonic velocities.

In short, following the obtained results, the Standard delta wing with LEX was the configuration with the lowest RCS signature. Likewise, this configuration presented adequate aerodynamic characteristics when comparing the analytical and numerical models.

Acknowledgments

The authors express their gratitude to Maria Luisa Bambozzi de Oliveira and Roberto Gil Annes da Silva, members of the evaluation Jury of the masters degree dissertation of Bravo-Mosquera P. D.

The authors are thankful to CAPES (Coordenação de Aperfeiçoamento de Pessoal de Nível Superior) for the scholarship granted.

References

- [1] Liangliang C, Kuizhi Y, Weigang G and Dazhao Y. Integration Analysis of Conceptual Design and Stealth-Aerodynamic Characteristics of Combat Aircraft. *Journal of Aerospace Technology and Management*. Vol. 8. No. 1, pp. 40-48. 2016.
- [2] Vaitheeswaran S, Gowthami T, Prasad S and Yathirajam B. Monostatic radar cross section of flying wing delta planforms. *Engineering Science and Technology, an International Journal*. Vol. 20. No. 2, pp. 467-481. 2017.

- [3] Lee M, Ho Chih-Ming. Lift force of delta wings. *Applied Mechanics Reviews*. Vol. 43. No. 9, pp. 209-221. 1990.
- [4] Bravo-Mosquera P D. Projeto conceitual e análise de desempenho do sistema de admissão de ar em uma aeronave não convencional de combate. *Dissertação de mestrado em Engenharia Mecânica*. Escola de Engenharia de São Carlos, Universidade de São Paulo. 2017.
- [5] Touzopoulos P, Boviatsis D and Zikidis K. 3D Modelling of potential targets for the purpose of radar cross section (RCS) prediction. *In: Proceedings of the 6th International Conference on Military Technologies (ICMT2017)*, Brno, Czech Republic. pp. 636-642. 2017.
- [6] Alves M, Port R, Rezende M. Simulations of the radar cross section of a stealth aircraft. *In: Microwave and Optoelectronics Conference*, 2007. *IMOC 2007. SBMO/IEEE MTT-S International. IEEE.* pp. 409-412. 2007.
- [7] Dos Santos L, De Andrade L, Gama A. Analysis of Radar Cross Section Reduction of Fighter Aircraft by Means of Computer Simulation. *Journal of Aerospace Technology and Management*. Vol. 6. No. 2. pp. 177-182, 2014.
- [8] Garrido E E. Graphical user interface for a physical optics radar cross section prediction code. *Doctoral dissertation, Monterey, California. Naval Postgraduate School.* 2000.
- [9] Chatzigeorgiadis F. Development of Code for a Physical Optics Radar Cross Section Prediction and Analysis Application. *Master Thesis*, *Naval Postgraduate School, Monterey, Califor*nia. 2004.
- [10] Barbosa U, Costa J, Munjulury R and Abdalla A. Analysis of Radar Cross Section and Wave Drag Reduction of Fighter Aircraft. In procedings of the AEROSPACE TECHNOLOGY CONGRESS 2016 Swedish aerospace technology in a globalised world. 2016.
- [11] Ghasemit A, Sousa E. Spectrum sensing in cognitive radio networks: requirements, challenges and design trade-offs. *IEEE Communications magazine*. Vol. 46. No. 4. 2008.
- [12] Raymer D. Aircraft design: A conceptual approach. *AIAA education series*. 1999.
- [13] Staack I, Munjulury R C, et al. Conceptual Design Model Management Demonstrated on a 4th

- Generation Fighter. *In: Proceedings of 29th International Council of the Aeronautical Science*. St. Petersberg, Russia. 2014.
- [14] Harris R V. An analysis and correlation of aircraft wave drag. NASATM X-947. National Technical Information Service, Hampton. 1964.
- [15] Hayes W D. Linearized supersonic flow. *PhD Thesis*. California Institute of Technology. 1947.

8 Contact Author Email Address

mailto: pdbravom@usp.br

Copyright Statement

The authors confirm that they, and/or their company or organization, hold copyright on all of the original material included in this paper. The authors also confirm that they have obtained permission, from the copyright holder of any third party material included in this paper, to publish it as part of their paper. The authors confirm that they give permission, or have obtained permission from the copyright holder of this paper, for the publication and distribution of this paper as part of the ICAS proceedings or as individual off-prints from the proceedings.